

9-2014

# A Selective NMR Probe to Monitor the Conformational Transition from Inactive to Active Kinase

Qian Xie  
*Iowa State University*

D. Bruce Fulton  
*Iowa State University, [bfulton@iastate.edu](mailto:bfulton@iastate.edu)*

Amy H. Andreotti  
*Iowa State University, [amyand@iastate.edu](mailto:amyand@iastate.edu)*

Follow this and additional works at: [http://lib.dr.iastate.edu/bbmb\\_ag\\_pubs](http://lib.dr.iastate.edu/bbmb_ag_pubs)



Part of the [Molecular Biology Commons](#)

The complete bibliographic information for this item can be found at [http://lib.dr.iastate.edu/bbmb\\_ag\\_pubs/25](http://lib.dr.iastate.edu/bbmb_ag_pubs/25). For information on how to cite this item, please visit <http://lib.dr.iastate.edu/howtocite.html>.

---

This Article is brought to you for free and open access by the Biochemistry, Biophysics and Molecular Biology at Digital Repository @ Iowa State University. It has been accepted for inclusion in Biochemistry, Biophysics and Molecular Biology Publications by an authorized administrator of Digital Repository @ Iowa State University. For more information, please contact [digirep@iastate.edu](mailto:digirep@iastate.edu).

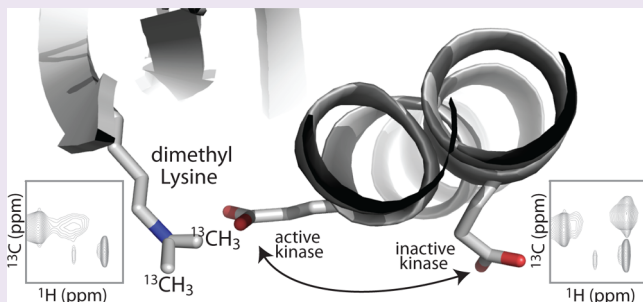
# A Selective NMR Probe to Monitor the Conformational Transition from Inactive to Active Kinase

Qian Xie, D. Bruce Fulton, and Amy H. Andreotti\*

Roy J. Carver Department of Biochemistry, Biophysics and Molecular Biology, Iowa State University, Ames, Iowa 50011, United States

## S Supporting Information

**ABSTRACT:** Kinases control many aspects of cellular signaling and are therefore therapeutic targets for numerous disease states. Monitoring the conformational changes that drive activation and inactivation of the catalytic kinase core is a challenging experimental problem due to the dynamic nature of these enzymes. We apply  $^{13}\text{C}$  reductive methylation to chemically introduce NMR-active nuclei into unlabeled protein kinases. The results demonstrate that solution NMR spectroscopy can be used to monitor specific changes in the chemical environment of structurally important lysines in a  $^{13}\text{C}$ -methylated kinase as it shifts from the inactive to active state. This approach provides a solution based method to complement X-ray crystallographic data and can be applied to nearly any kinase, regardless of size or method of production.



Kinase inhibitor development<sup>1,2</sup> has driven significant investment in understanding the precise structural features that control kinase activity. Most of our knowledge regarding kinase structure comes from X-ray crystallography, a technique that provides spectacular views of the molecular determinants that control the catalytic activity of these enzymes.<sup>3–5</sup> Despite its power to resolve atomic level details, X-ray diffraction captures static structural snapshots; the intermediates along the trajectory of a conformational transition are often lost. Moreover, use of X-ray crystallography to solve numerous drug or ligand bound structures can be laborious or not feasible. To complement and enhance available X-ray derived structural information, solution-based techniques must continue to be developed to adequately interrogate kinase structure–function relationships.

Here we report a simple and rapid NMR approach to assess the conformational preferences of any kinase in solution. Using  $^{13}\text{C}$ -labeled formaldehyde, we have used reductive methylation chemistry<sup>6</sup> to introduce a spectroscopic probe into the active site at the  $\beta 3$  strand lysine of a model kinase. The chemical environment surrounding the  $\beta 3$  lysine changes on transition from inactive to active kinase,<sup>7–9</sup> providing a direct reporter of the activation trajectory. The method can be applied to any kinase regardless of expression system and creates a novel platform to study kinase regulatory mechanisms under a range of solution conditions. In addition to providing insight into how exogenous proteins and/or second messengers affect kinase regulation, the method can be used to directly measure the effect of disease-causing mutations or small molecule modulators on the conformational preferences of the kinase active site.

Src tyrosine kinase was chosen as a model system for NMR method development due to its well understood regulatory mechanism.<sup>10</sup> The Src domain structure consists of two Src Homology domains, SH3 and SH2, a catalytic kinase domain and a C-terminal tail containing a regulatory tyrosine (Tyr527) (Figure 1a). In the autoinhibited conformation of Src,<sup>11,12</sup> phosphorylated Tyr527 binds to the Src SH2 domain intramolecularly and the Src SH3 domain interacts with the linker spanning the SH2 and kinase domains (Figure 1b). Dephosphorylation of Tyr527, and/or exogenous ligand binding to SH3 and SH2, liberates the kinase domain from the conformational restraints imposed by the SH3/2 domains, and the kinase domain shifts to the active conformation<sup>13–17</sup> (Figure 1b). It is also established that the isolated kinase domains of Src family members (lacking the SH3-SH2 region) are active.<sup>18</sup>

Kinases share the  $\beta 3$  strand lysine in the N-lobe that protrudes toward the active site, coordinates ATP, and forms a salt bridge with the conserved glutamate on the C-helix. In crystal structures of the autoinhibited form of Src,<sup>12</sup> the C-helix is out of the active site, and the distance between the Lys  $\epsilon$ -amine group and the Glu carboxylate group (Lys295/Glu310) is 14 Å (Figure 1c). In structures of active Src,<sup>19</sup> the C-helix abuts the active site of the kinase domain leading to a short, 3.7 Å, distance between the Lys295 and Glu310 side chains (Figure 1d). The chemical environment of Lys295 differs between

**Special Issue:** New Frontiers in Kinases

**Received:** June 12, 2014

**Accepted:** September 23, 2014

**Published:** September 23, 2014

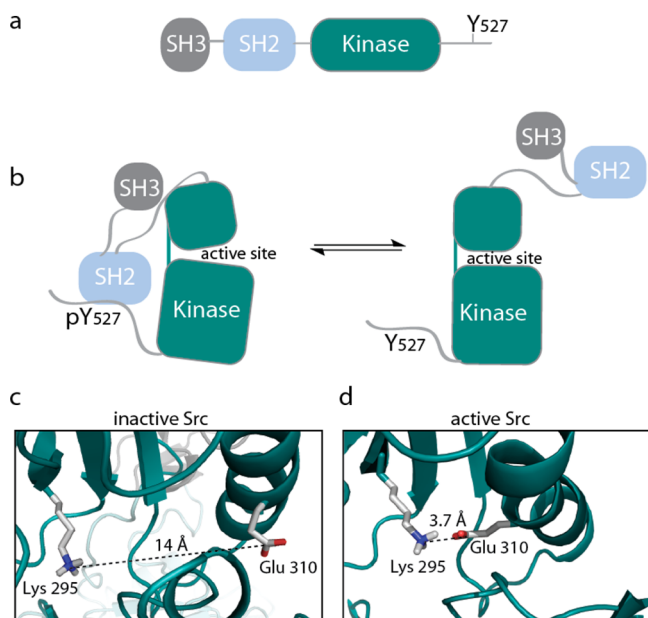


**Figure 1.** Src structure. (a) Src kinase domain structure. (b) Schematic of the conformational equilibrium between inactive (left) and active (right) states. (c) Crystal structure of the inactive Src kinase (2SRC) showing the conserved Lys295 and Glu310. (d) Crystal structure of the active Src kinase (1Y57) showing the short distance between Lys295 and Glu310.

active and inactive conformations, and NMR chemical shift can therefore serve as a reporter of kinase activation status.

The  $\epsilon$ -NH<sub>3</sub><sup>+</sup> protons of lysine are not good NMR probes due to rapid exchange with water and resulting unfavorable relaxation properties. However, if the lysine side chain is modified in a manner that introduces a nonexchangeable NMR probe and retains the electrostatic properties of the native side chain, the conformational transitions between active and inactive kinases could be monitored in solution. Protein reductive methylation results in two methyl groups covalently attached to the  $\epsilon$ -NH<sub>2</sub> of lysine side chains as well as the amino terminal  $\alpha$ -NH<sub>2</sub> (Figure 2a, inset).<sup>6</sup> The positive charge on the lysine side chain is maintained, and so ion pair interactions are largely maintained.<sup>20</sup> The favorable relaxation properties of CH<sub>3</sub> allow NMR analysis of both conformationally constrained and mobile lysine side chains.<sup>21–23</sup>

Two forms of the Src kinase, SH3-SH2-kinase domain (SH3SH2KD) and the isolated Src kinase domain (KD), were expressed and purified to homogeneity (Supplementary Figure S1a). We use a modified form of Src SH3SH2KD that contains a tail sequence optimized for intramolecular SH2 binding favoring the inactive conformation.<sup>24</sup> We subjected Src SH3SH2KD and Src KD to reductive methylation by [<sup>13</sup>C]-labeled formaldehyde using ammonia borane as the reducing agent.<sup>25</sup> SDS-PAGE, MALDI-TOF mass spectrometry, and MS/MS analysis were used to characterize the methylated Src SH3SH2KD and KD proteins and confirmed dimethylation of primary amines and Lys295 in particular (Supplementary Figure S1a,b). Circular dichroism (CD) spectra for the methylated and unmethylated Src SH3SH2KD and KD proteins are similar (Supplementary Figure S1c,d), indicating methylation does not affect secondary structural elements. Moreover, methylation of <sup>15</sup>N-labeled Src KD allowed acquisition of a <sup>1</sup>H–<sup>15</sup>N heteronuclear single quantum coherence (HSQC) spectrum of the modified protein.

Comparison of this two-dimensional NMR data set with that of unmethylated, <sup>15</sup>N-labeled Src kinase domain shows that almost all resonances overlap for the two proteins, and only a small subset of peaks resonate at different frequencies, consistent with the overall kinase domain fold remaining intact following lysine methylation (Supplementary Figure S1e).

Kinase activity of methylated Src was dramatically reduced compared to unmodified enzymes (Supplementary Figure S2a). The loss of activity is likely due to impaired ATP coordination in the active site, since in addition to its interaction with Glu310, the  $\beta$ 3 strand Lys295 coordinates the  $\alpha$ - and  $\beta$ -phosphates of ATP. Indeed, addition of the stable ATP analogue, AMP-PNP, to <sup>15</sup>N-labeled samples of unmodified and methylated Src KD shows loss of binding to the methylated protein at concentrations that match the ATP concentration used in the activity assays (Supplementary Figure S2b,c). There is ample precedence, most notably in the pseudokinase literature,<sup>26</sup> for catalytically incompetent kinases being able to populate both active and inactive conformations. Moreover, inactive kinases are often employed for biophysical experiments,<sup>7,27</sup> and so, despite the loss of catalytic activity for the methylated kinase, we proceeded with analysis using NMR spectroscopy.

We acquired a [<sup>1</sup>H,<sup>13</sup>C] HSQC spectrum for the [<sup>13</sup>C]-methylated Src SH3SH2KD protein (Figure 2a). This experiment measures the <sup>1</sup>H and <sup>13</sup>C resonance frequencies of each [<sup>13</sup>C] C–H functional group. A number of <sup>1</sup>H–<sup>13</sup>C crosspeaks are evident in the spectrum and correspond to the methyl resonances of the dimethylated lysine side chains and to concentrated buffer components due to <sup>13</sup>C at natural abundance. Based on previously published work,<sup>20</sup> the dimethyl resonances are centered at a <sup>13</sup>C chemical shift of ~45 ppm. The dimethyl peaks that resonate downfield in the <sup>1</sup>H dimension are largely degenerate and likely correspond to methyl groups attached to solvent-exposed lysines that experience similar chemical environments (Figure 2b). In contrast, several methyl resonances are well-resolved and shifted upfield, suggesting the presence of unique lysine side chain environments within Src.

Assignment of the  $\beta$ 3 strand lysine (Lys295 in Src) was accomplished by mutation of Lys295 to methionine in the Src SH3SH2KD protein. Methylation of the mutant protein followed by acquisition of the [<sup>1</sup>H,<sup>13</sup>C] HSQC spectrum revealed a single missing resonance that is assigned to Lys295 in the original spectrum (Figure 2b,c). Additional peaks are shifted upfield in the <sup>1</sup>H dimension, suggesting that at least one other lysine residue exists in a unique environment. Systematic mutation of candidate lysines, followed by methylation and acquisition of [<sup>1</sup>H,<sup>13</sup>C] HSQC data for each mutant, led to assignment of the <sup>1</sup>H–<sup>13</sup>C cross peak at 2.25 and 42.5 ppm as dimethylated Lys315 (Figure 2b,d). The dimethylated  $\alpha$ -NH<sub>2</sub> was assigned by introducing a thrombin cleavage site between the N-terminal hexaHis tag and the first residue of Src SH3SH2KD. The methylated protein was then treated with thrombin and further purified using a Ni resin to remove uncleaved protein and the resulting His tag peptide. The [<sup>1</sup>H,<sup>13</sup>C] HSQC spectrum for Src SH3SH2KD lacking the N-terminus reveals a single missing resonance, allowing unequivocal assignment of the dimethylated amino-terminus ( $\alpha$ -NH<sub>2</sub>) (Figure 2b,e). The same mutagenesis approach was used to assign the corresponding resonances in the [<sup>1</sup>H,<sup>13</sup>C] HSQC spectrum of Src KD (Supplementary Figure S3).

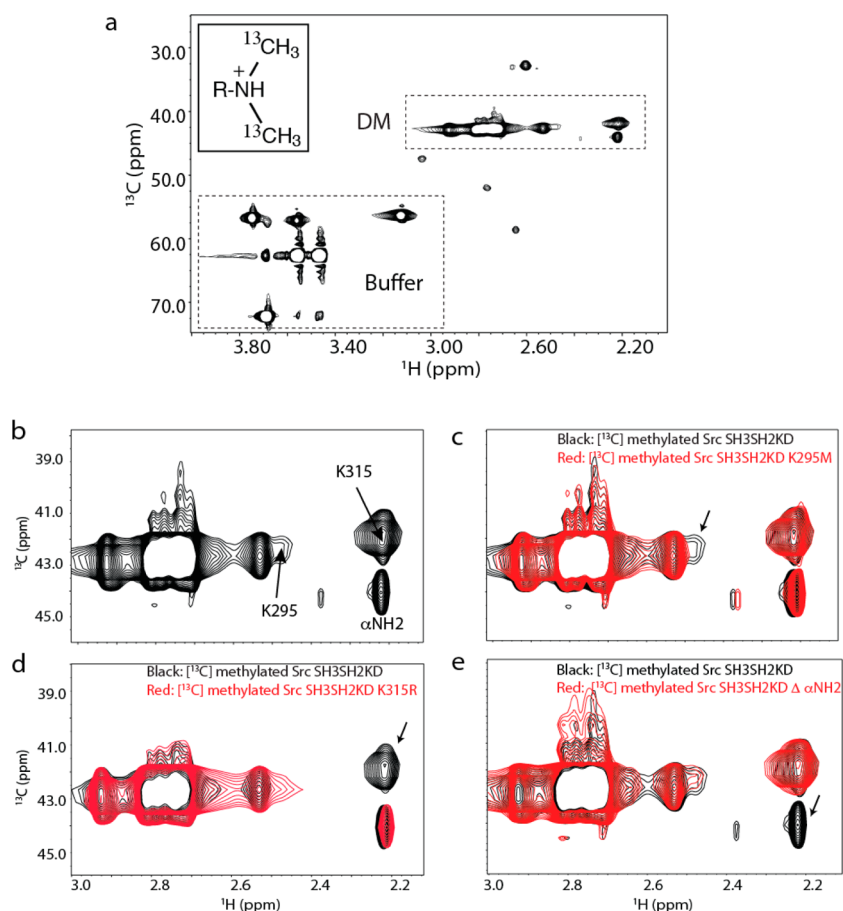


**Figure 2.** Chemical modification and NMR data acquisition and assignment. (a)  $^1\text{H}$ ,  $^{13}\text{C}$  HSQC spectrum of  $^{13}\text{C}$ -methylated Src SH3SH2KD. Dimethylated lysine resonances are labeled “DM”, and NMR signals from buffer components are labeled (identified by acquiring the identical  $^1\text{H}$ ,  $^{13}\text{C}$  HSQC spectrum on buffer alone). The inset shows the structure of the protonated, dimethyl lysine epsilon amino group. (b) Select region of the  $^1\text{H}$ ,  $^{13}\text{C}$  HSQC spectrum of methylated Src SH3SH2KD. Dimethyl Lys295, Lys315, and the dimethylated amino terminus ( $\alpha\text{NH}_2$ ) are assigned on the basis of mutational data shown in panels c–e. (c–e) Superposition of  $^1\text{H}$ ,  $^{13}\text{C}$  HSQC spectra of  $^{13}\text{C}$ -methylated SH3SH2KD (black) and Lys295Met mutant (red) (c); Lys315Arg mutant (red) (d); and SH3SH2KD lacking the amino-terminus (e). In panels c–e the missing resonance in the mutant spectrum is indicated by the arrow.

The resolved methyl resonances of Lys295 and 315 provide two separate probes within the Src SH3SH2KD protein to monitor conformational changes during the course of Src activation. Lys315 is one and a half turns away from Glu310 on the C-helix and in the autoinhibited Src structure projects away from the N-lobe of the kinase domain toward the linker between SH2 and kinase domains, making extensive contacts with Trp260 (Figure 3a). Src activation leads to a large shift in the position of the SH3/SH2 domains and the SH2-kinase linker region (Figure 3b). Peptide ligands that target the Src SH3 and/or SH2 domains compete with the autoinhibited form and activate the Src kinase.<sup>28</sup> We titrated two peptides, VSLARRPLPLP and pYEEIE (ligands for the Src SH3 and SH2 domains, respectively), into the NMR sample containing  $^{13}\text{C}$ -methylated Src SH3SH2KD (Figure 3c,d). Addition of increasing concentration of SH3 ligand causes spectral changes; specifically, the peak corresponding to Lys295 disappears over the course of SH3 ligand titration, due to line broadening and/or chemical shift change that results in overlap with the neighboring peak (Figure 3c). The Lys315 methyl peak exhibits slow exchange behavior as SH3 ligand concentration increases (Figure 3c). Saturation with SH3 peptide ligand results in the emergence of a new peak at a  $^1\text{H}$  frequency of 2.28 ppm and

complete loss of the original Lys315 signal present in the spectrum of free Src SH3SH2KD.

In a separate titration, the SH2 peptide ligand, pYEEIE, was added to the methylated Src SH3SH2KD sample. Stepwise addition of the pYEEIE peptide causes no spectral change over a range of ligand concentrations (Supplementary Figure S4). This result can be reconciled with the fact that we are using a modified Src construct that contains a high affinity tail sequence surrounding pTyr527; the isolated pYEEIE phosphopeptide does not compete with the intramolecular ligand for SH2 binding at the concentrations used in the NMR experiment. We therefore explored whether the pYEEIE ligand might compete with the pTyr527 for binding to the SH2 domain of SH3SH2KD in the context of SH3 peptide ligand. Using the SH3SH2KD sample that is already saturated with SH3 ligand (last panel in Figure 3c), we added increasing concentration of the pYEEIE peptide. In this titration, addition of SH2 ligand results in further chemical shift perturbation of the Lys315 methyl resonance (Figure 3d). The finding that ligand occupancy of the SH3 domain in SH3SH2KD affects accessibility of the SH2 domain in the intact Src protein is reminiscent of crosstalk between regulatory domains explored previously using other methods.<sup>29–32</sup>



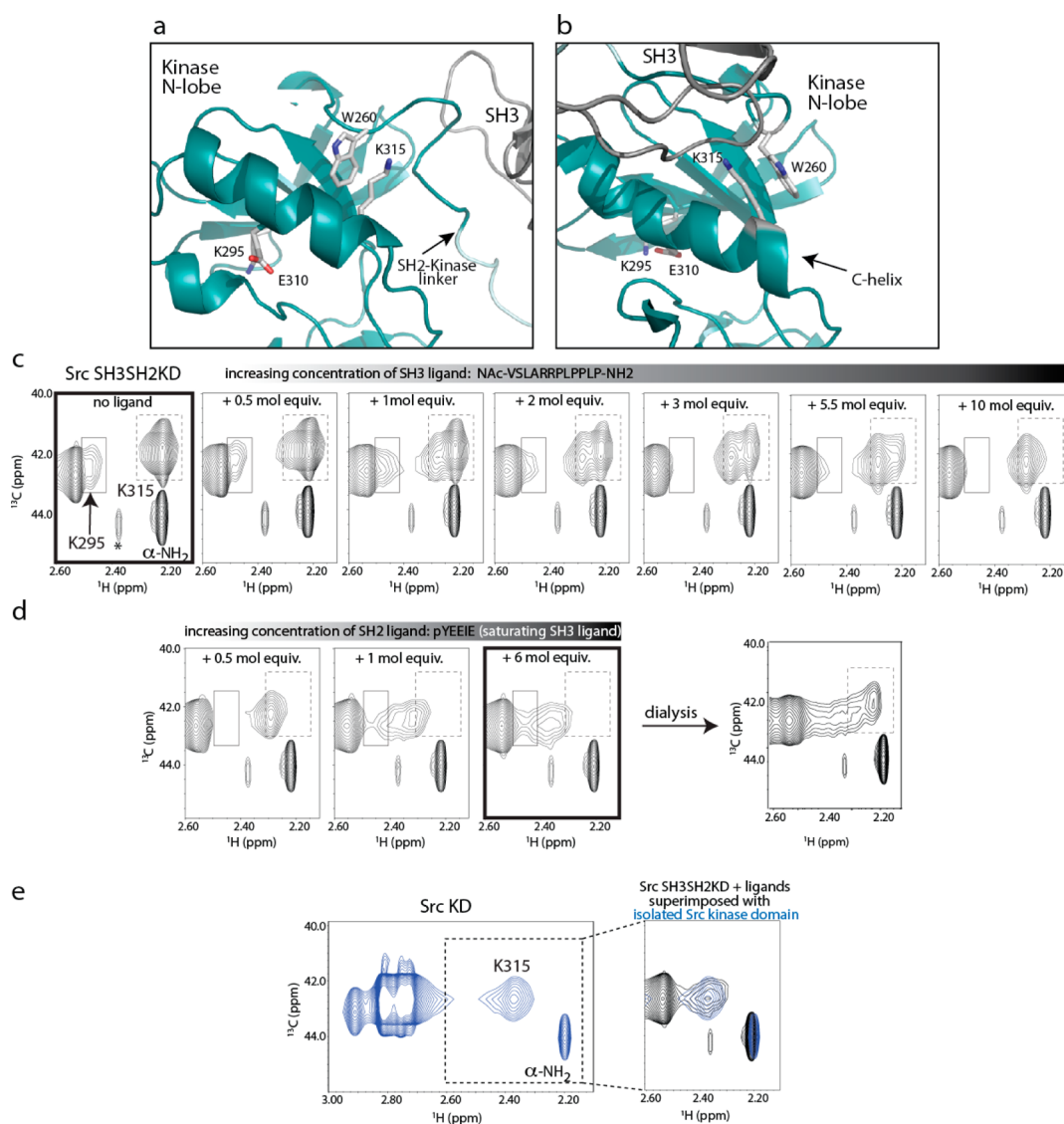


**Figure 3.** Conformational transition from inactive to active Src monitored by NMR. (a,b) Structures of (a) inactive Src (2SRC) and (b) active Src (1Y57) showing Lys295 and Lys315 in the N-lobe of the kinase domain. Glu310 and Trp260 are also shown, as are portions of the SH3 and SH2 domains on the “backside” of the Src kinase domain. (c) SH3 peptide ligand (NAC-VSLARRPLPLP-NH<sub>2</sub>) was titrated into 135  $\mu\text{M}$  [ $^{13}\text{C}$ ]-methylated Src SH3SH2KD, and [ $^1\text{H}$ , $^{13}\text{C}$ ] HSQC spectra were acquired at each titration point. The left-most spectrum is [ $^{13}\text{C}$ ]-methylated Src SH3SH2KD with no ligand (bold outline), and the following six spectra contain increasing molar equivalents of peptide ligand. Boxes throughout panels c and d show the resonance frequencies of Lys295 and Lys315 in the absence of ligand. Peak assignments are indicated in the first spectrum, and the asterisk indicates an unidentified peak. (d) SH2 peptide ligand (Caffeic acid-pYEEIE) titrated into the [ $^{13}\text{C}$ ]-methylated Src SH3SH2KD sample containing 10 molar equiv of SH3 peptide ligand (last panel in part c). The bolded spectrum is Src SH3SH2KD protein in the presence of saturating amounts of both SH3 and SH2 domain ligands. The final panel shows the spectrum acquired after dialysis of the ligand-saturated Src SH3SH2KD sample. (e) (left) [ $^1\text{H}$ , $^{13}\text{C}$ ] HSQC spectrum of the [ $^{13}\text{C}$ ]-methylated Src kinase domain (Src KD). (right) Superposition of the Src KD spectrum (blue) with the [ $^1\text{H}$ , $^{13}\text{C}$ ] HSQC spectrum of SH3SH2KD after saturation with both SH3 and SH2 ligands (black).

Upon saturation of SH3SH2KD with both SH3 and SH2 ligands, the dimethyl lysine region differs dramatically from the [ $^1\text{H}$ , $^{13}\text{C}$ ] HSQC spectrum acquired for free SH3SH2KD (Figure 3c,d (bolded spectra)). Superposition of the SH3/SH2 ligand-saturated SH3SH2KD spectrum with that of the isolated Src kinase domain (KD) shows an exact correspondence in the resolved region (Figure 3e). This finding provides direct evidence that SH3 and SH2 ligand binding results in release of the Src kinase domain, which then adopts the active conformation present in the free kinase domain. Finally, we subjected the ligand-saturated SH3SH2KD sample to repeated dialysis to remove peptide ligands and determine the reversibility of the conformational shift. Acquisition of a

[ $^1\text{H}$ , $^{13}\text{C}$ ] HSQC spectrum following dialysis shows that the resonance belonging to Lys315 reappears at its original chemical shift (Figure 3d), suggesting that reduced peptide ligand binding to the SH3 and SH2 domains leads to a conformational shift toward the inactive conformation.

The proof-of-principle experiment in Figure 3 demonstrates that NMR spectroscopy, using [ $^{13}\text{C}$ ]-methylated lysine side chains as probes, reports on the conformational ensemble of the Src kinase domain under a range of conditions. In light of the inconvenient exchange regime/chemical shift degeneracy of the Lys295 resonance, the well-resolved Src Lys315 peak provides a convenient, alternative signal that monitors the complete conformational transition between inactive and active

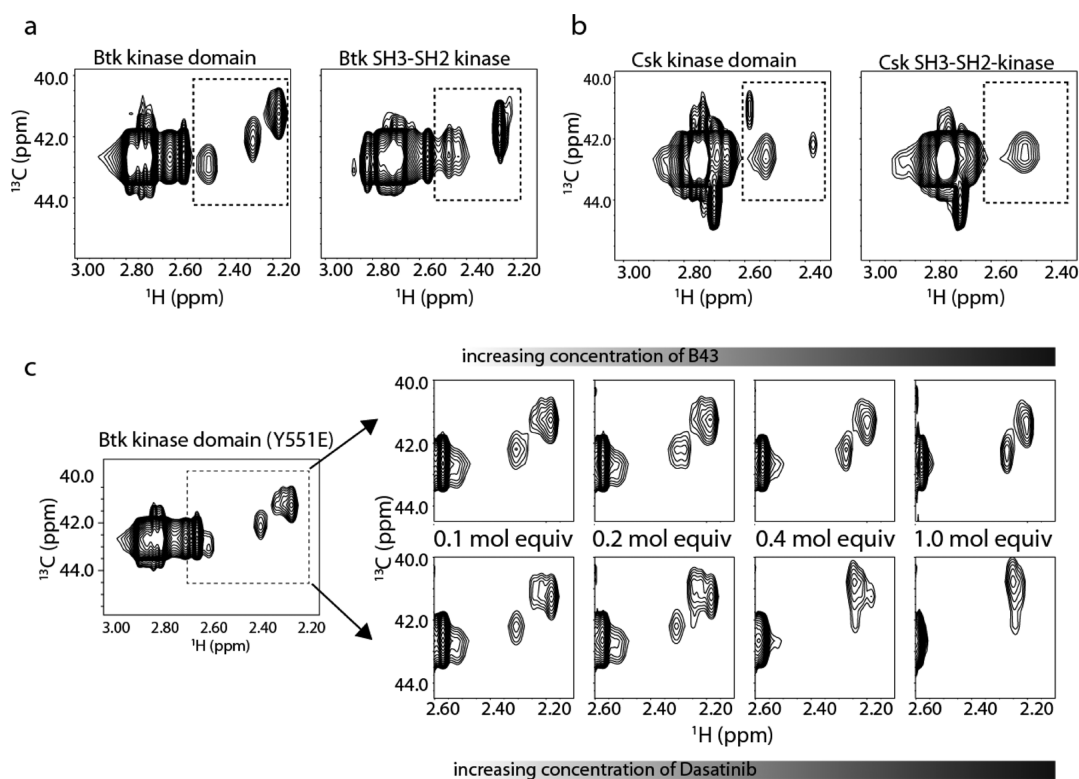


**Figure 4.** Extension of method to additional kinases. (a,b) Dimethyl lysine region of spectra acquired for [ $^{13}\text{C}$ ]-methylated Btk (a) and Csk (kinase domains and SH3-SH2-kinase domain constructs) (b). Non-degenerate resonances are indicated with a dashed box. (c) Btk kinase domain drug titrations. A 100  $\mu\text{M}$  sample of [ $^{13}\text{C}$ ]-methylated Btk kinase domain (Tyr551 is mutated to Glu to correspond to protein used in the reported crystal structure<sup>35</sup>) was titrated with either B43 (top row) or dasatinib (bottom row) at the indicated molar equivalents. [ $^1\text{H}$ ,  $^{13}\text{C}$ ] HSQC spectra shown are acquired before addition of drug or at each titration point. The Btk kinase domain also carries the Y617P mutation that facilitates bacterial expression.<sup>39</sup>

Src (Figure 3c,d). While Src Lys315 is not strictly conserved across kinase families, we wondered whether other kinases would similarly exhibit multiple resolved dimethyl lysine resonances that, in the event of unfavorable spectral properties for the conserved  $\beta 3$  lysine, could be used to monitor the complete conformational transition between inactive and active kinase. To this end, we expressed and purified two additional kinases, Btk and Csk, and subjected these proteins to reductive methylation. Acquisition of [ $^1\text{H}$ ,  $^{13}\text{C}$ ] HSQC spectra for methylated Btk and Csk (Figure 4a,b) shows that these kinases, like Src, exhibit multiple nondegenerate dimethyl resonances. Moreover, a comparison of the isolated Btk and Csk kinase domains to their corresponding multidomain proteins (SH3SH2KD) shows spectral differences in the region of the resolved dimethyl lysine resonances (Figure 4a,b) consistent with activity differences, and hence conformational differences, in the kinase domain induced by the presence of the non-catalytic domains.<sup>33,34</sup> While residue-specific assignments and characterization of these systems are beyond the scope of the current work, these data suggest that the presence of multiple spectroscopic probes may be a general feature of reductively methylated kinases.

We next took advantage of two Btk inhibitors, B43 and dasatinib; both bind to the kinase active site yet stabilize distinct conformational states. X-ray crystallography has shown that binding of B43 stabilizes the kinase inactive conformation, while dasatinib stabilizes the active state.<sup>35</sup> We titrated these small molecules into separate samples of the [ $^{13}\text{C}$ ]-methylated Btk KD and acquired [ $^1\text{H}$ ,  $^{13}\text{C}$ ] HSQC spectra at increasing

concentrations of inhibitor (Figure 4c,d). The resulting series of spectra indicate that the resolved dimethyl lysine resonances are sensitive to inhibitor binding in the Btk active site. Moreover, the end points of the two titrations are different, suggesting that B43 and dasatinib favor different kinase domain conformational states in solution consistent with the co-crystal structures.<sup>35</sup> These data suggest that, in addition to allosteric modulators (Figure 3), reagents that target the kinase active site can also be assessed using the combination of  $^{13}\text{C}$  reductive lysine methylation and NMR spectroscopy described here. It should be noted, however, that the proximity of the  $\beta 3$  lysine to the kinase active site means that its dimethyl resonance frequency may be affected by both the conformational changes induced within the kinase domain and direct binding of the inhibitor, complicating spectral analysis. For this reason, the presence of an alternative dimethyl lysine peak outside of the active site, such as Lys315 in Src, may be particularly valuable in studies focused on active site inhibitors.

In conclusion, NMR data acquired using a lysine methylated sample provide a spectral signature of the Src kinase activation/inactivation trajectory. The data report on the conformational ensemble that is present in solution, enabling the identification of intermediates along the course of kinase activation. We suggest this method will allow investigators to gain insight into the conformational ensemble of any pharmaceutically important, full-length protein kinase in solution, many of which rely on eukaryotic expression systems for production, are difficult to isotopically label, and show limited yield. The approach can be used to assess how allosteric and direct interactions, between a

kinase and its binding partner, be it a substrate, a regulator, or an adaptor protein, drives the conformation of the kinase domain toward the active or inactive state. Similarly, the method provides a rapid analysis of conformational status of a kinase upon inhibition with a small molecule, complementing previous applications of  $^{13}\text{C}$  NMR spectroscopy to kinase drug discovery.<sup>36</sup> Finally, insight into how specific disease-causing mutations within or outside of a kinase domain affect conformational preferences of the catalytic site can also be gained with this method. Overall, this method promises to provide deeper insight into the molecular basis of kinase regulatory mechanisms.

## METHODS

**Protein Production.** Src proteins were coexpressed with YopH and purified as described.<sup>37</sup>  $^{15}\text{N}$ -Labeled proteins were expressed in minimal media as described previously.<sup>38</sup> Reductive methylation followed previous published protocols.<sup>25</sup> All mutations were introduced using site-directed mutagenesis kit (Stratagene) and verified by sequencing at the ISU DNA Synthesis and Sequencing Facility.

**Characterization of Methylated Kinases.** For trypsin digestion, 15  $\mu\text{L}$  of 50 mM  $\text{NH}_4\text{HCO}_3$  and 1.5  $\mu\text{L}$  of 100 mM DTT were added to 10  $\mu\text{L}$  of 0.8 mg/mL kinase sample, and the volume was adjusted to 27  $\mu\text{L}$  with  $\text{H}_2\text{O}$ . The mixture was incubated at 95  $^\circ\text{C}$  for 5 min, and 3  $\mu\text{L}$  of 100 mM iodoacetamide was added and incubated in the dark at RT for 20 min. Next, 1  $\mu\text{L}$  of sequencing grade modified trypsin (Promega) at 0.1  $\mu\text{g}/\mu\text{L}$  was added and incubated for 3 h at 37  $^\circ\text{C}$ . Digested samples were analyzed by MALDI-TOF and MS/MS using Q-Star XL quadrupole-TOF tandem mass spectrometer (ABI) in the Protein Facility at Iowa State University. Initial velocities for Src KD and SH3SH2KD (methylated and unmethylated) were measured using a generic peptide substrate, poly(Glu,Tyr), as previously described.<sup>34</sup>

**NMR Spectroscopy.** NMR spectra were acquired at 25  $^\circ\text{C}$  on a Bruker AVII700 spectrometer with a 5 mm HCN z-gradient cryoprobe operating at  $^1\text{H}$  frequency of 700.13 MHz using standard protocols (Bruker pulse program hsqcetgppsp.2 and troyf3gppsi19). Sample concentration was 135  $\mu\text{M}$  ( $^{13}\text{C}$ ]-methylated Src SH3SH2KD and KD) or 200  $\mu\text{M}$  (methylated and unmethylated  $^{15}\text{N}$ ]-Src KD) in the following buffer: 50 mM bicine pH 8.0, 100 mM NaCl, 2 mM DTT, 5% glycerol, and 0.02%  $\text{NaN}_3$ . SH3 ligand VSLARRPLPLP was purchased from GenScript, and SH2 ligand Caffeic acid-pYEEIE was from Tocris Bioscience. The  $^{13}\text{C}$  reductively methylated Src SH3SH2KD titration sample was dialyzed against 500 mL of buffer (50 mM bicine pH 8.0, 100 mM NaCl, 2 mM DTT, 5% glycerol, 0.02%  $\text{NaN}_3$ ), changed each day for 7 days prior to acquisition of the  $^{1}\text{H}$ ,  $^{13}\text{C}$ ] HSQC spectrum. For AMP-PNP binding experiments,  $\text{MgCl}_2$  was added to the  $^{15}\text{N}$ -labeled Src KD samples (methylated and unmethylated) to a final concentration of 10 mM. B43 was purchased from Calbiochem and dasatinib was purchased from Selleckchem.

## ASSOCIATED CONTENT

### Supporting Information

Additional characterization of the reductively methylated proteins used in this study, as well as further information on resonance assignments, ATP binding, and ligand titration. This material is available free of charge via the Internet at <http://pubs.acs.org>.

## AUTHOR INFORMATION

### Corresponding Author

\*E-mail: amyand@iastate.edu.

### Notes

The authors declare no competing financial interest.

## ACKNOWLEDGMENTS

We thank T. Smithgall for providing the Src and YopH constructs and R. Joseph for useful discussions and careful reading of the manuscript. This work is supported by a grant from the National Institutes of Health (NIAID, AI043957) to A.H.A.

## REFERENCES

- (1) Deininger, M. W., and Druker, B. J. (2003) Specific targeted therapy of chronic myelogenous leukemia with imatinib. *Pharmacol. Rev.* 55, 401–423.
- (2) Zhang, J., Yang, P. L., and Gray, N. S. (2009) Targeting cancer with small molecule kinase inhibitors. *Nat. Rev. Cancer* 9, 28–39.
- (3) Cowan-Jacob, S. W. (2006) Structural biology of protein tyrosine kinases. *Cell. Mol. Life Sci.* 63, 2608–2625.
- (4) Taylor, S. S., Ilouz, R., Zhang, P., and Kornev, A. P. (2012) Assembly of allosteric macromolecular switches: lessons from PKA. *Nat. Rev. Mol. Cell Biol.* 13, 646–658.
- (5) Breitenlechner, C. B., Bossemeyer, D., and Engh, R. A. (2005) Crystallography for protein kinase drug design: PKA and SRC case studies. *Biochim. Biophys. Acta* 1754, 38–49.
- (6) Means, G. E., and Feeney, R. E. (1968) Reductive alkylation of amino groups in proteins. *Biochemistry* 7, 2192–2201.
- (7) Iyer, G. H., Garrod, S., Woods, V. L., Jr., and Taylor, S. S. (2005) Catalytic independent functions of a protein kinase as revealed by a kinase-dead mutant: study of the Lys72His mutant of cAMP-dependent kinase. *J. Mol. Biol.* 351, 1110–1122.
- (8) Iyer, G. H., Moore, M. J., and Taylor, S. S. (2005) Consequences of lysine 72 mutation on the phosphorylation and activation state of cAMP-dependent kinase. *J. Biol. Chem.* 280, 8800–8807.
- (9) Jura, N., Zhang, X., Endres, N. F., Seeliger, M. A., Schindler, T., and Kuriyan, J. (2011) Catalytic control in the EGF receptor and its connection to general kinase regulatory mechanisms. *Mol. Cell* 42, 9–22.
- (10) Boggon, T. J., and Eck, M. J. (2004) Structure and regulation of Src family kinases. *Oncogene* 23, 7918–7927.
- (11) Xu, W., Doshi, A., Lei, M., Eck, M. J., and Harrison, S. C. (1999) Crystal structures of c-Src reveal features of its autoinhibitory mechanism. *Mol. Cell* 3, 629–638.
- (12) Xu, W., Harrison, S. C., and Eck, M. J. (1997) Three-dimensional structure of the tyrosine kinase c-Src. *Nature* 385, 595–602.
- (13) Engen, J. R., Wales, T. E., Hochrein, J. M., Meyn, M. A., 3rd, Banu Ozkan, S., Bahar, I., and Smithgall, T. E. (2008) Structure and dynamic regulation of Src-family kinases. *Cell. Mol. Life Sci.* 65, 3058–3073.
- (14) Cooper, J. A., and Howell, B. (1993) The when and how of Src regulation. *Cell* 73, 1051–1054.
- (15) Gonfloni, S., Williams, J. C., Hattula, K., Weijland, A., Wierenga, R. K., and Superti-Furga, G. (1997) The role of the linker between the SH2 domain and catalytic domain in the regulation and function of Src. *EMBO J.* 16, 7261–7271.
- (16) Sicheri, F., and Kuriyan, J. (1997) Structures of Src-family tyrosine kinases. *Curr. Opin. Struct. Biol.* 7, 777–785.
- (17) Moarefi, I., LaFevre-Bernt, M., Sicheri, F., Huse, M., Lee, C. H., Kuriyan, J., and Miller, W. T. (1997) Activation of the Src-family tyrosine kinase Hck by SH3 domain displacement. *Nature* 385, 650–653.
- (18) Veillette, A., Caron, L., Fournel, M., and Pawson, T. (1992) Regulation of the enzymatic function of the lymphocyte-specific tyrosine protein kinase p56lck by the non-catalytic SH2 and SH3 domains. *Oncogene* 7, 971–980.
- (19) Cowan-Jacob, S. W., Fendrich, G., Manley, P. W., Jahnke, W., Fabbro, D., Liebetanz, J., and Meyer, T. (2005) The crystal structure of a c-Src complex in an active conformation suggests possible steps in c-Src activation. *Structure* 13, 861–871.

- (20) Jentoft, J. E., Jentoft, N., Gerken, T. A., and Dearborn, D. G. (1979)  $^{13}\text{C}$  NMR studies of ribonuclease A methylated with [ $^{13}\text{C}$ ]Formaldehyde. *J. Biol. Chem.* 254, 4366–4370.
- (21) Nicholson, L. K., Kay, L. E., Baldissari, D. M., Arango, J., Young, P. E., Bax, A., and Torchia, D. A. (1992) Dynamics of methyl groups in proteins as studied by proton-detected  $^{13}\text{C}$  NMR spectroscopy. Application to the leucine residues of staphylococcal nuclease. *Biochemistry* 31, 5253–5263.
- (22) Bokoch, M. P., Zou, Y., Rasmussen, S. G., Liu, C. W., Nygaard, R., Rosenbaum, D. M., Fung, J. J., Choi, H. J., Thian, F. S., Kobilka, T. S., Puglisi, J. D., Weis, W. I., Pardo, L., Prosser, R. S., Mueller, L., and Kobilka, B. K. (2010) Ligand-specific regulation of the extracellular surface of a G-protein-coupled receptor. *Nature* 463, 108–112.
- (23) Chavan, T. S., Abraham, S., and Gaponenko, V. (2013) Application of reductive ( $^{13}\text{C}$ )-methylation of lysines to enhance the sensitivity of conventional NMR methods. *Molecules* 18, 7103–7119.
- (24) Porter, M., Schindler, T., Kuriyan, J., and Miller, W. T. (2000) Reciprocal regulation of Hck activity by phosphorylation of Tyr(527) and Tyr(416). Effect of introducing a high affinity intramolecular SH2 ligand. *J. Biol. Chem.* 275, 2721–2726.
- (25) Abraham, S. J., Hoheisel, S., and Gaponenko, V. (2008) Detection of protein-ligand interactions by NMR using reductive methylation of lysine residues. *J. Biomol. NMR* 42, 143–148.
- (26) Zeqiraj, E., and van Aalten, D. M. (2010) Pseudokinases-remnants of evolution or key allosteric regulators? *Curr. Opin. Struct. Biol.* 20, 772–781.
- (27) Opatowsky, Y., Lax, I., Tome, F., Bleichert, F., Unger, V. M., and Schlessinger, J. (2014) Structure, domain organization, and different conformational states of stem cell factor-induced intact KIT dimers. *Proc. Natl. Acad. Sci. U.S.A.* 111, 1772–1777.
- (28) Yadav, S. S., and Miller, W. T. (2007) Cooperative activation of Src family kinases by SH3 and SH2 ligands. *Cancer Lett.* 257, 116–123.
- (29) Hochrein, J. M., Lerner, E. C., Schiavone, A. P., Smithgall, T. E., and Engen, J. R. (2006) An examination of dynamics crosstalk between SH2 and SH3 domains by hydrogen/deuterium exchange and mass spectrometry. *Protein Sci.* 15, 65–73.
- (30) Alvarado, J. J., Betts, L., Moroco, J. A., Smithgall, T. E., and Yeh, J. I. (2010) Crystal structure of the Src family kinase Hck SH3-SH2 linker regulatory region supports an SH3-dominant activation mechanism. *J. Biol. Chem.* 285, 35455–35461.
- (31) Lerner, E. C., and Smithgall, T. E. (2002) SH3-dependent stimulation of Src-family kinase autophosphorylation without tail release from the SH2 domain in vivo. *Nat. Struct. Biol.* 9, 365–369.
- (32) Lerner, E. C., Tribble, R. P., Schiavone, A. P., Hochrein, J. M., Engen, J. R., and Smithgall, T. E. (2005) Activation of the Src family kinase Hck without SH3-linker release. *J. Biol. Chem.* 280, 40832–40837.
- (33) Joseph, R. E., Min, L., and Andreotti, A. H. (2007) The Linker between SH2 and Kinase Domains Positively Regulates Catalysis of the Tec Family Kinases. *Biochemistry* 46, 5455–5462.
- (34) Joseph, R. E., Xie, Q., and Andreotti, A. H. (2010) Identification of an allosteric signaling network within Tec family kinases. *J. Mol. Biol.* 403, 231–242.
- (35) Marcotte, D. J., Liu, Y. T., Arduini, R. M., Hession, C. A., Miatkowski, K., Wildes, C. P., Cullen, P. F., Hong, V., Hopkins, B. T., Mertsching, E., Jenkins, T. J., Romanowski, M. J., Baker, D. P., and Silvan, L. F. (2010) Structures of human Bruton's tyrosine kinase in active and inactive conformations suggest a mechanism of activation for TEC family kinases. *Protein Sci.* 19, 429–439.
- (36) Comess, K. M., Sun, C., Abad-Zapatero, C., Goedken, E. R., Gum, R. J., Borhani, D. W., Argiriadi, M., Groebe, D. R., Jia, Y., Clampit, J. E., Haasch, D. L., Smith, H. T., Wang, S., Song, D., Coen, M. L., Cloutier, T. E., Tang, H., Cheng, X., Quinn, C., Liu, B., Xin, Z., Liu, G., Fry, E. H., Stoll, V., Ng, T. I., Banach, D., Marcotte, D., Burns, D. J., Calderwood, D. J., and Hajduk, P. J. (2011) Discovery and characterization of non-ATP site inhibitors of the mitogen activated protein (MAP) kinases. *ACS Chem. Biol.* 6, 234–244.
- (37) Seeliger, M. A., Young, M., Henderson, M. N., Pellicena, P., King, D. S., Falick, A. M., and Kuriyan, J. (2005) High yield bacterial expression of active c-Abl and c-Src tyrosine kinases. *Protein Sci.* 14, 3135–3139.
- (38) Brazin, K. N., Fulton, D. B., and Andreotti, A. H. (2000) A specific intermolecular association between the regulatory domains of a Tec family kinase. *J. Mol. Biol.* 302, 607–623.
- (39) Xie, Q., Joseph, R. E., Fulton, D. B., and Andreotti, A. H. (2013) Substrate recognition of PLCgamma1 via a specific docking surface on Itk. *J. Mol. Biol.* 425, 683–696.